Chemistry Research Journal, 2017, 2(1):1-11

Available online www.chemrj.org

Research Article

ISSN: 2455-8990
CODEN(USA): CRJHA5

A Quantum Chemical Analysis of the Relationships between Electronic Structure and the inhibition of Botulinum Neurotoxin serotype A by a series of Derivatives possessing an 8-hydroxyquinoline core

Juan S. Gómez-Jeria*, Julio César Surco-Luque

Quantum Pharmacology Unit, Department of Chemistry, Faculty of Sciences, University of Chile. Las Palmeras 3425, Santiago 7800003, Chile

Abstract A formal analysis of the relationships between electronic structure and inhibition of the Botulinum neurotoxin serotype A by a series of derivatives possessing an 8-hydroxyquinoline core was carried out. The wave functions were calculated at the B3LYP/6-31G(d,p) level after full geometry optimization. A statistically significant equation relating five specific local atomic indices with inhibitory capacity was obtained. The variation of the inhibitory ability seems to be orbital-controlled. From the analysis of the resulting equation, a partial inhibitory pharmacophore was built, summarizing those atomic sites that could be substituted to obtain molecules with enhanced inhibitory capability.

Keywords Biological warfare, neurotoxins, QSAR, electronic structure, botulinum, DFT

Introduction

Biological warfare has a long history [1-4]. Among these warfare agents, botulinum toxins are the most lethal toxins known, with an LD_{50} of 10–13 ng/kg when inhaled. Because botulinum toxin is so deadly and easy to produce and weaponize, it represents a more than credible menace. The Japanese Empire military fed their war prisoners with *C. botulinum* cultures in the 1930s and the Japanese sect Aum Shinrikyō ("Supreme Truth") tried to release an airborne form of botulinum toxin on three occasions during the early 1990s, but all of the attacks failed. Saddam Hussein was in possession of about 19,000 L of concentrated botulinum toxin, enough to kill the whole human population three times by inhalation. Botulinum toxins, anthrax and Ebola and influenza viruses are probably the choice weapons for bioterrorism and for countries not interested in fabricating chemical or nuclear weapons because of satellite surveillance. We note that Ebola viruses can be obtained directly in Africa and that, in the case of the 1918 flu pandemic, the original virus can be easily isolated from the bodies of frozen victims.

There are seven types of botulinum toxins (named types A–G). Type A and B cause disease in humans. One of them, botulinum neurotoxin serotype A (BoNT/A), is composed by a ~100 kDa heavy chain (HC) attached via a single disulfide Cys-Cys bond to a ~50 kDa light chain (LC).Given this situation, all studies contributing to understand the action of compounds inhibiting BoNT/A should be welcome. Several groups of molecules inhibiting BoNT/A have been synthesized and tested [5-19]. In two earlier papers we studied the inhibition of the BoNT/A light chain (BoNT/A LC) by some 1,7-bis-(amino alkyl)diazachrysene derivatives and also the inactivation rate constant of the BoNT/A LC by some 1,4-benzoquinone and 1,4-naphthoquinone derivatives [20-21]. In a third paper we analyzed the inhibitory activity of a large group of 8-hydroxy-quinolines tested in the SNAPtide assay (this assay allows the identification of BoNT/A LC inhibitors) [22- 23]. This was complemented with a docking analysis of the

R and S isomers. In that paper we concluded that "*We can see that R and S isomers seem to dock to the binding site in very different forms. Therefore, any experimental study of any biological activity of these compounds cannot be done with the racemic mixture*" [22].

Recently, a new experimental report, about the inhibition of BoNT/A LC by some quinolinol derivatives, was published [24]. Here we present the results of a density functional study of the relationships between the electronic structure and the inhibitory capacity of these compounds.

Methods, Models and Calculations

The molecules studied here act as inhibitors of BoNT/A LC and have an 8-hydroxyquinoline core. They were selected from a recent study [24]. Their general formula and biological activity are displayed, respectively, in Fig. 1 and Table 1.

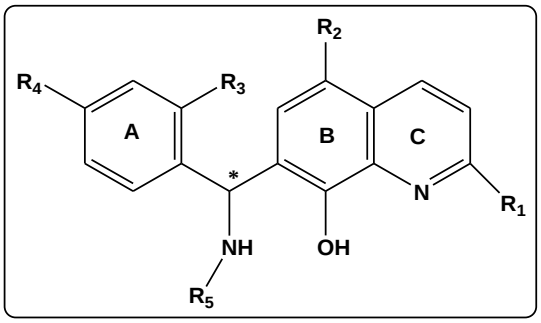

Figure 1: General formula of the molecules analyzed here

Table 1: Molecules and their biological activity

Molecule	R_1	R_2	R_3	R_4	R_5	$\log(IC_{50})$
1	H	H	H	H	2-pyridyl	0.18
2	H	H	F	H	3-pyridyl	0.38
3	H	Cl	H	H	2-pyridyl	0.18
4	H	H	H	H	3-pyridyl	0.79
5	H	H	H	H	2-pyrimidyl	0.43
6	H	H	F	H	2-pyridyl	0.08
7	H	H	F	H	2-pyrimidyl	0.28
8	H	H	H	F	2-pyridyl	0.61
9	H	H	H	F	3-pyridyl	0.66
10	H	H	H	F	2-pyrimidyl	0.23
11	H	H	F	F	2-pyridyl	0.56
12	H	H	F	F	3-pyridyl	0.64
13	H	H	F	F	2-pyrimidyl	1.10
14	Me	H	H	H	2-pyridyl	-0.15
15	Me	H	H	H	3-pyridyl	0.15
16	Me	H	H	H	2-pyrimidyl	0.66
17	Me	H	F	H	2-pyridyl	0.15
18	Me	H	F	H	3-pyridyl	-0.15
19	Me	H	F	H	2-pyrimidyl	1.08
20	Me	H	H	F	2-pyridyl	0.20
21	Me	H	H	F	3-pyridyl	-0.10
22	Me	H	H	F	2-pyrimidyl	0.62
23	Me	H	F	F	2-pyridyl	0.43
24	Me	H	F	F	3-pyridyl	1.09
25	Me	H	F	F	2-pyrimidyl	0.63
26	H	Cl	H	H	3-pyridyl	0.54
27	H	Cl	H	H	2-pyrimidyl	0.65

28	H	Cl	F	H	2-pyridyl	0.15
29	H	Cl	F	H	3-pyridyl	-0.15
30	H	Cl	F	H	2-pyrimidyl	0.60
31	H	Cl	H	F	2-pyridyl	-0.22
32	H	Cl	H	F	3-pyridyl	0.36
33	H	Cl	H	F	2-pyrimidyl	-0.15
34	H	Cl	F	F	2-pyridyl	-0.15
35	H	Cl	F	F	3-pyridyl	-0.22
36	H	Cl	F	F	2-pyrimidyl	0.34

The method employed here, called the Klopman-Peradejordi-Gómez or KPG method, has been explained in a several papers [25-30] and here we shall only discuss the results. It is only member of the class of model-based methods [31]. It was initially developed for drug-site affinity constants [32] but later it was concluded that it can be employed for all kinds of biological activities [33]. Its success is beyond all reasonable doubts (see [34-60] and references therein).

The electronic structure of all molecules was calculated within the Density Functional Theory (DFT) at the B3LYP/6-31g(d,p) level with full geometry optimization [61]. The Gaussian set of programs was used [62] was obtained from the Gaussian results with the D-Cent-QSAR software [63]. All electron populations smaller than or equal to 0.01 e were considered as zero [29]. Negative electron populations coming from Mulliken Population Analysis were corrected as usual [64]. Orientational parameter values were taken from Tables [65]. As the solving of the system of linear equations is not possible for the reason that we have not enough molecules, we made use of Linear Multiple Regression Analysis (LMRA) techniques to find the best solution. A matrix containing the dependent variable ($\log(IC_{50})$) and the local atomic reactivity indices of all atoms of the common skeleton plus the orientational parameters of the R_1-R_5 substituents as independent variables was constructed. The Statistica software was used for LMRA [66].

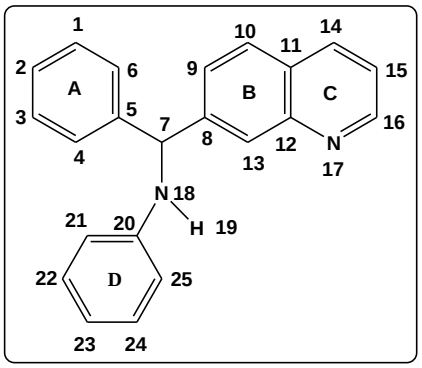

Figure 2: Common skeleton numbering

We worked with the *common skeleton hypothesis* stating that there is a definite collection of atoms, common to all molecules analyzed, that accounts for nearly all the biological activity. The action of the substituents consists in modifying the electronic structure of the common skeleton and influencing the right alignment of the drug throughout the orientational parameters. It is hypothesized that different parts or this common skeleton accounts for almost all the interactions leading to the expression of a given biological activity. The common skeleton is shown in Fig. 2.

Results

The best equation obtained is:

$$\log(IC_{50}) = 1.97 + 0.81S^{E}_{23}(HOMO)^{*} - 0.02S^{N}_{10}(LUMO+2)^{*} + \\ +2.67F_{20}(LUMO+1)^{*} - 1.45F_{11}(HOMO)^{*} - 0.72F_{2}(LUMO)^{*} \quad (1)$$

with n =27, R= 0.95, R^2= 0.91, adjusted R^2= 0.89, F(5,21)=42.120 (p<0.000001) and a Std. error of estimate of 0.12. No outliers were detected and no residuals fall outside the ±2σ limits. Here, S_{23}^{E}(HOMO)* is the electrophilic superdelocalizability of the highest occupied MO localized on atom 23, S_{10}^{N}(LUMO+2)* is the nucleophilic superdelocalizability of the third lowest empty MO localized on atom 10, F_{20}(LUMO+1)* is the electron population of the second lowest empty MO localized on atom 20, F_{11}(HOMO)* is the electron population of the highest occupied MO localized on atom 11 (The Fukui index, [67]) and F_2(LUMO) is the electron population of the lowest empty MO localized on atom 2.

Tables 2 and 3 show the beta coefficients, the results of the t-test for significance of coefficients and the matrix of squared correlation coefficients for the variables of Eq. 1. There are no significant internal correlations between independent variables (Table 3). Figure 3 displays the plot of observed *vs.* calculated log(IC_{50}).

Table 2: Beta coefficients and t-test for significance of coefficients in Eq. 1

	Beta	**t(21)**	**p-level**
S_{23}^{E}(HOMO)*	0.45	5.98	<0.000006
S_{10}^{N}(LUMO+2)*	-0.55	-7.92	<0.000001
F_{20}(LUMO+1)*	0.65	9.05	<0.000001
F_{11}(HOMO)*	-0.35	-4.95	<0.00007
F_2(LUMO)	-0.27	-3.57	<0.0018

Table 3: Matrix of squared correlation coefficients for the variables in Eq. 1

	S_{23}^{E}(HOMO)*	**S_{10}^{N}(LUMO+2)***	**F_{20}(LUMO+1)***	**F_{11}(HOMO)***
S_{10}^{N}(LUMO+2)*	0.01	1.00		
F_{20}(LUMO+1)*	0.03	0.04	1.00	
F_{11}(HOMO)*	0.02	0.03	0.12	1.00
F_2(LUMO)	0.03	0.01	0.02	0.11

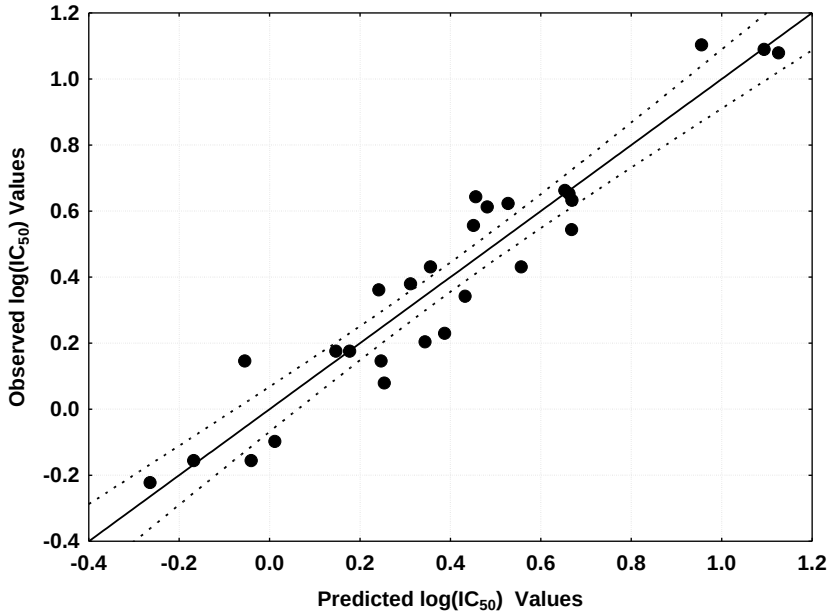

Figure 3: Plot of predicted vs. observed log(IC_{50}) values (Eq. 1). Dashed lines denote the 95% confidence interval

The associated statistical parameters of Eq. 1 indicate that this equation is statistically significant and that the variation of the numerical values of a group of five local atomic reactivity indices of atoms of the common skeleton explains about 89% of the variation of $\log(IC_{50})$. Figure 3, spanning about 1.6 orders of magnitude, shows that there is a good correlation of observed *versus* calculated values (see below).

Local Molecular Orbitals

Tables 4 and 5 show the Local Molecular Orbitals of atoms 2, 10, 11, 20 and 23 (Eq. 1). Nomenclature: Molecule (molecule's HOMO) / (HOMO-2)* (HOMO-1)* (HOMO)* - (LUMO)* (LUMO+1)* (LUMO+2)*.

Table 4: Local Molecular Orbitals of atoms 2, 10 and 11 (Eq. 1)

Molecule	Atom 2	Atom 10	Atom 11
1(82)	78π80π81π-86π87π88π	80π81π82π-83π87π88π	79π81π82π-84π85π87π
2(86)	81π82π86π-88π89π91π	81π83π85π-87π93π94σ	83π84π85π-88π89π90π
3(90)	87π88π89π-94π95π96π	88π89π90π-91π92π94π	87π88π90π-92π95π96π
4(82)	78π79σ82π-84π85π86π	77π80π81π-83π84π89π	79π80π81π-84π85π86π
5(82)	79π80π81π-86π87π88π	80π81π82π-83π85π88π	80π81π82π-85π88π89π
6(86)	84π85π86π-88π89π90π	82σ84π85π-87π93π94π	84σ85π86π-88π89π90π
7(86)	84π85π86π-88π89π90π	84σ85π86π-87π93π94π	83π84σ86π-89π90π91π
8(86)	82π83π85π-90π91π92π	81σ84π86π-87π93π94π	83π85π86π-88π89π90π
9(86)	83π84π86π-88π89π90π	81σ84π85π-87π88π93π	82π84π85π-88π89π90π
10(86)	82σ83π85π-90π91π92π	81σ84π86π-87π89π93π	82π85π86π-89π90π91π
11(90)	88π89π90π-92π93π94π	86σ88σ89π-91π97π98π	88σ89π90π-92π93π94π
12(90)	85π86π90π-92π94π95π	86σ87π89π-91π97π98π	87π88π89π-92π93π95π
13(90)	87π88π90π-92π93π94π	88σ89π90σ-91π97π98π	87π88π90π-93π94π96π
14(86)	82π84π85π-90π91π92π	84π85π86π-87π89π92σ	84π85π86π-88π89π91π
15(86)	81π82π86π-88π89π90π	81σ82σ85π-87π88π93π	82σ83π84π-88π89π90π
16(86)	82π84π85π-90π91π92π	84π85π86π-87π89π92π	84π85π86π-89π92π93π
17(90)	88π89π90π-92π93π94π	87π88π89π-91π97π98π	87π88π90π-92π93π94π
18(90)	85π86π90π-92π93π94π	82π86σ89-91π97π98π	86σ87π88π-92π93π94π
19(90)	87π88π90π-92π93π94π	88π89π90π-91π97π98π	87π88π90π-93π94π95π
20(90)	87π88π89π-94π95π96π	88π89σ90π-91π93π97π	87π89π90π-92π93π94π
21(90)	86π88π90π-92π93π94π	82π85σ89π-91π92π97π	86σ87π88π-92π93π94π
22(90)	87π88π89π-94π95π96π	88π89π90π-91π93π97π	87π89π90π-93π94π95π
23(94)	92π93π94π-96π97π98π	91π92π93π-95π101π102π	91π92π94π-96π97π98π
24(94)	88π89π94π-96π97π98π	86π90σ93π-95π97π101π	90σ91π92π-96π97π99π
25(94)	91π92π94π-96π97π98π	91π93π94π-95π97π101π	91π92π94π-97π98π100π
26(90)	85π87π90π-92π93π94π	82π84σ89π-91π92π95π	87σ88π89π-92π94π95π
27(90)	87π88π89π-94π95π96π	88π89π90π-91π93π94σ	87π88σ90π-93π96π97π
28(94)	92π93π94π-96π98π99π	89σ92π93π-95π101π102σ	90π91π93π-96π97π98π
29(94)	88π91π94π-96π97π98π	89σ90π93π-95π101π102σ	90π91σ93π-96π97π99π
30(94)	88π92π94π-96π97π98π	92π93π94π-95π101π102σ	90π91π94π-97π98π101π
31(94)	92π93π94π-96π98π99π	89σ92π93π-95π101π102σ	90σ91π93π-96π97π98π
32(94)	88π91π94π-96π97π98π	89π90π93π-95π101π102σ	90π91σ93π-96π97π99π
33(94)	88π92π94π-96π97π98π	92π93π94π-95π101π102σ	90π91π94π-97π98π101π
34(98)	96π97π98π-100π102π103π	94σ96σ97π-99π105π106σ	95π96σ97π-100π101π102π
35(98)	94π95π98π-100π101π102π	90π93σ97π-99π100π105π	94π95π97π-100π101π103π
36(98)	95π96π98π-100π101π102π	96π97π98π-99π105π106π	95π97π98π-101π102π104π

Table 4: Local Molecular Orbitals of atoms 20 and 21 (Eq. 1).

Molecule	Atom 20	Atom 23
1(82)	80π81σ82π-84π85π86π	80π81π82π-84π85π86π
2(86)	83σ84σ86π-88π89π90π	83π84π86π-88π89π90π
3(90)	88σ89π90π-93π94π95π	88π89π90π-93π94π95π
4(82)	79σ80σ82π-85π86σ88σ	79π80π82π-85π86π88π
5(82)	80σ81σ82π-84π85π86π	80π81π82π-84π85π86π
6(86)	81σ84σ86π-88π89π90π	83π84π86π-89π90π91π
7(86)	84σ85π86π-88π90π91π	84π85π86π-88π90π91π
8(86)	84σ85σ86π-88π89π90π	84π85π86π-88π89π90π
9(86)	83σ84σ86π-89π90π91σ	83π84π86π-89π90π91π
10(86)	84π85σ86π-88π89π90π	84π85π86π-88π89π90π
11(90)	84σ88σ90π-93π95π96π	88π89π90π-93π95π96π
12(90)	87σ88σ90π-94π95π96σ	87π88π90π-94π95π96π
13(90)	88σ89π90π-92π94π95π	88π89π90π-92π94π95π
14(86)	84σ85σ86π-88π89π90π	84π85π86π-88π89π90π
15(86)	83σ84σ86π-89π90σ92σ	83π84π86π-89π90π92π
16(86)	84σ85σ86π-88π89π90π	84π85π86π-88π89π90π
17(90)	85σ88σ90π-92π93π94π	87π88π90π-93π94π95π
18(90)	87σ88σ90π-92π93σ94σ	87π88π90π-92π93π94π
19(90)	88σ89π90π-92π94π95π	88π89π90π-92π94π95π
20(90)	87σ89σ90π-92π94π95π	88π89π90π-92π93π94π
21(90)	87σ88σ90π-93π94σ95σ	87π88π90π-93π94π95π
22(90)	88σ89σ90π-92π93π94π	88π89π90π-92π93π94π
23(94)	91σ92σ94π-96π97π99π	91π92π94π-97π99π100π
24(94)	91σ92σ94π-98π100σ102σ	91π92π94π-98π100π106π
25(94)	92σ93π94π-96π98π99π	92π93π94π-96π98π99π
26(90)	87σ88σ90π-93π94σ96σ	87π88π90π-93π94π96π
27(90)	88σ89σ90π-92π93σ94π	88π89π90π-92π93π94π
28(94)	91σ92σ94π-97π98π99π	91π92π94π-97π98π99π
29(94)	88σ92σ94π-97π98σ100σ	91π92π94π-97π98π100π
30(94)	92σ93π94π-96π98π99π	92π93π94π-96π98π99π
31(94)	91σ92σ94π-97π98π99π	91σ92σ94π-97π98π99π
32(94)	88σ92σ94π-97π98π100σ	91π92σ94π-97π98π100π
33(94)	92σ93π94π-96π98π99π	92σ93π94π-96π98π99π
34(98)	93σ96σ98π-100π101π103σ	93σ96σ98π-101π103π104π
35(98)	95σ96σ98π-102π103π104σ	95σ96σ98π-102π103π104π
36(98)	96σ97π98π-100π102π103π	96π97π98π-100π102π103π

Discussion

Table 2 shows that the importance of variables in Eq. 1 is F_{20}(LUMO+1)*> S_{10}^{N}(LUMO+2)*> S_{23}^{E}(HOMO)*> F_{11}(HOMO)*> F_2(LUMO).A high inhibitory activity is associated with large negative values of S_{23}^{E}(HOMO)*, large positive values of F_{11}(HOMO)* and F_2(LUMO) and small positive values of F_{20}(LUMO+1)*. If the numerical values of S_{10}^{N}(LUMO+2)* are positive, a high inhibitory activity is associated with large numerical values. Atom 20 is a carbon in ring D (Fig. 2). $(LUMO+1)_{20}$* has a π or σ nature (Table 4). $(LUMO)_{20}$* has a π nature in all molecules and also participates in the inhibitory process. Table 4 shows also that $(LUMO)_{20}$* does not coincide with

the molecule's HOMO. Considering that a high inhibitory capacity is associated with small positive values of F_{20}(LUMO+1)* and that the plot of F_{20}(LUMO)* vs. inhibitory activity (not shown here) shows a similar trend, we suggest that molecules in which the lowest empty MO localized on atom 20 located energetically far from the molecule's LUMO would be a good inhibitor. This suggests that atom 20 is acting as an electron donor. Atom 10 is a carbon in ring B (Fig. 2). Table 4 shows that $(LUMO)_{10}$* and $(LUMO+1)_{10}$* have a π nature, while $(LUMO+2)_{10}$* has π or σ natures. A high inhibitory activity is associated with large numerical values for S_{10}^{N}(LUMO+2)* for positive values of this index. To get larger values we must shift downwards the corresponding eigenvalue, making this MO more reactive. Other possibility is to increase the Fukui index (with values in the [0,2] interval). Therefore, the ideal situation is when the first three lowest empty MOs have a π nature and coincide with the first three lowest empty MOs of the molecule. Therefore, atom 10 acts as an electron acceptor. Atom 23 is a carbon in ring D (Fig. 2). Eq. 1 says that large negative values of S_{23}^{E}(HOMO)* are associated with a high inhibitory activity. Table 4 shows that $(HOMO)_{23}$* has a π nature. Larger negative values are obtained by shifting upwards the energy of the associated eigenvalue. This makes this MO more susceptible to act as an electron donor. Atom 11 is a carbon in rings B-C (Fig. 2). Table 4 shows that $(HOMO)_{11}$* has a π nature. As larger positive values of F_{11}(HOMO)* are associated with higher inhibitory activity, we conclude that atom 11 is acting as an electron donor. Atom 2 is a carbon in ring A (Fig. 2). Table 4 shows that $(LUMO)_2^*$ has a π nature. As large positive values of F_2(LUMO)* are associated with high inhibitory activity, we suggest that atom 2 is acting as an electron acceptor. All the above suggestions are displayed in the partial 2D pharmacophore of Fig. 4.

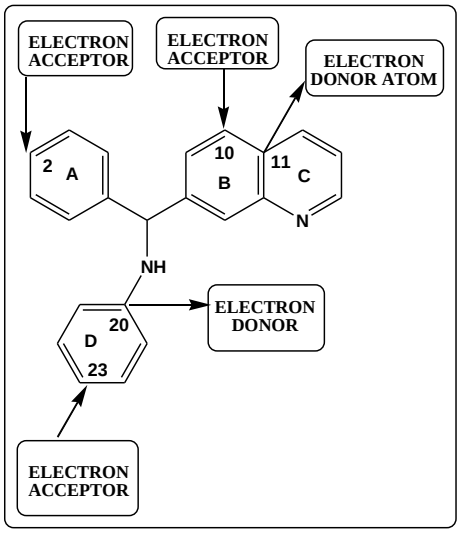

Figure 4: 2D pharmacophore for the inhibition of BoNT/A

All rings A-D seem to participate in the inhibitory process. The previous analysis strongly suggests that atoms in Eq.1 interact with the site through π-π weak bonds and that the inhibitory process is orbital-controlled [68-69]. Despite the good results obtained here, we must insist that measuring the activity of a racemic mixture is a totally incorrect approach. Perhaps this is the reason why many points in Fig. 3 are outside the 95% confidence interval. Anyway the pharmacophore displays some atomic sites that can be modified to obtain improved inhibitors.

In conclusion, a good relationship between the electronic structure and BoNT/A LC inhibition has been obtained for the abovementioned series, showing again that the KPG method is superior to the methods based only on statistics.

References

1. Freney, J.; Renaud, F.o. *Microbes at war : from the Dark Ages to modern times*. Eska Pub.: Paris, France ; Portland, Ore., 2011.
2. Spiers, E.M. *A history of chemical and biological weapons*. Reaktion: London, 2010.

3. Nie, J.-B. *Japan's wartime medical atrocities: comparative inquiries in science, history, and ethics*. Routledge: London ; New York, 2010.
4. Williams, P.; Wallace, D. *Unit 731: Japan's secret biological warfare in World War II*. 1st American ed.; Free Press: New York, 1989.
5. Čapková, K.; Yoneda, Y.; Dickerson, T.J.; Janda, K.D. Synthesis and structure–activity relationships of second-generation hydroxamate botulinum neurotoxin A protease inhibitors. *Bioorganic & Medicinal Chemistry Letters* **2007,** 17, 6463-6466.
6. Silvaggi, N.R.; Boldt, G.E.; Hixon, M.S.; Kennedy, J.P.; Tzipori, S.; Janda, K.D.; Allen, K.N. Structures of Clostridium botulinum Neurotoxin Serotype A Light Chain Complexed with Small-Molecule Inhibitors Highlight Active-Site Flexibility. *Chemistry & Biology* **2007,** 14, 533-542.
7. Čapková, K.; Salzameda, N.T.; Janda, K.D. Investigations into small molecule non-peptidic inhibitors of the botulinum neurotoxins. *Toxicon* **2009,** 54, 575-582.
8. Lai, H.; Feng, M.; Roxas-Duncan, V.; Dakshanamurthy, S.; Smith, L.A.; Yang, D.C.H. Quinolinol and peptide inhibitors of zinc protease in botulinum neurotoxin A: Effects of zinc ion and peptides on inhibition. *Archives of Biochemistry and Biophysics* **2009,** 491, 75-84.
9. Moe, S.T.; Thompson, A.B.; Smith, G.M.; Fredenburg, R.A.; Stein, R.L.; Jacobson, A.R. Botulinum neurotoxin serotype A inhibitors: Small-molecule mercaptoacetamide analogs. *Bioorganic & Medicinal Chemistry* **2009,** 17, 3072-3079.
10. Li, B.; Cardinale, S.C.; Butler, M.M.; Pai, R.; Nuss, J.E.; Peet, N.P.; Bavari, S., et al. Time-dependent botulinum neurotoxin serotype A metalloprotease inhibitors. *Bioorganic & Medicinal Chemistry* **2011,** 19, 7338-7348.
11. Opsenica, I.; Filipovic, V.; Nuss, J.E.; Gomba, L.M.; Opsenica, D.; Burnett, J.C.; Gussio, R., et al. The synthesis of 2,5-bis(4-amidinophenyl)thiophene derivatives providing submicromolar-range inhibition of the botulinum neurotoxin serotype A metalloprotease. *European Journal of Medicinal Chemistry* **2012,** 53, 374-379.
12. Smith, G.R.; Caglič, D.; Čapek, P.; Zhang, Y.; Godbole, S.; Reitz, A.B.; Dickerson, T.J. Reexamining hydroxamate inhibitors of botulinum neurotoxin serotype A: Extending towards the β-exosite. *Bioorganic & Medicinal Chemistry Letters* **2012,** 22, 3754-3757.
13. O'Malley, S.; Sareth, S.; Jiao, G.-S.; Kim, S.; Thai, A.; Cregar-Hernandez, L.; McKasson, L., et al. Virtual medicinal chemistry: In silico pre-docking functional group transformation for discovery of novel inhibitors of botulinum toxin serotype A light chain. *Bioorganic & Medicinal Chemistry Letters* **2013,** 23, 2505-2511.
14. Šilhár, P.; Silvaggi, N.R.; Pellett, S.; Čapková, K.; Johnson, E.A.; Allen, K.N.; Janda, K.D. Evaluation of adamantane hydroxamates as botulinum neurotoxin inhibitors: Synthesis, crystallography, modeling, kinetic and cellular based studies. *Bioorganic & Medicinal Chemistry* **2013,** 21, 1344-1348.
15. Zuniga, J.; Hammill, J.; Drory, O.; Nuss, J.; Burnett, J.; Gussio, R.; Wipf, P., et al. Structural basis for the inhibition of botulinum neurotoxin serotype A by potent peptidomimetics. *Toxicon* **2013,** 68, 103-104.
16. Bremer, P.T.; Hixon, M.S.; Janda, K.D. Benzoquinones as inhibitors of botulinum neurotoxin serotype A. *Bioorganic & Medicinal Chemistry* **2014,** 22, 3971-3981.
17. Seki, H.; Pellett, S.; Šilhár, P.; Stowe, G.N.; Blanco, B.; Lardy, M.A.; Johnson, E.A., et al. Synthesis/biological evaluation of hydroxamic acids and their prodrugs as inhibitors for Botulinum neurotoxin A light chain. *Bioorganic & Medicinal Chemistry* **2014,** 22, 1208-1217.
18. Kumaran, D.; Adler, M.; Levit, M.; Krebs, M.; Sweeney, R.; Swaminathan, S. Interactions of a potent cyclic peptide inhibitor with the light chain of botulinum neurotoxin A: Insights from X-ray crystallography. *Bioorganic & Medicinal Chemistry* **2015,** 23, 7264-7273.

19. Teng, Y.-H.G.; Berger, W.T.; Nesbitt, N.M.; Kumar, K.; Balius, T.E.; Rizzo, R.C.; Tonge, P.J., et al. Computer-aided identification, synthesis, and biological evaluation of novel inhibitors for botulinum neurotoxin serotype A. *Bioorganic & Medicinal Chemistry* **2015,** 23, 5489-5495.
20. Gómez-Jeria, J.S.; Robles-Navarro, A. A Quantum Chemical Analysis of the Inactivation Rate Constant of the BoNT/A LC Neurotoxin by some 1,4-Benzoquinone and 1,4-Naphthoquinone derivatives. *Journal of Computational Methods in Molecular Design* **2015,** 5, 15-26.
21. Gómez-Jeria, J.S. A Preliminary Formal Quantitative Structure-Activity Relationship Study of some 1,7-Bis-(amino alkyl)diazachrysene Derivatives as Inhibitors of Botulinum Neurotoxin Serotype A Light Chain and Three P. falciparum Malaria Strains. *Journal of Computational Methods in Molecular Design* **2014,** 4, 32-44.
22. Gómez-Jeria, J.S.; Reyes-Díaz, I.; Valdebenito-Gamboa, J. Quantum-Chemical and Docking Studies of 8-Hydroxy-Quinolines as Inhibitors of the Botulinum Neurotoxin A Light Chain (BoNT/A LC). *Journal of Computational Methods in Molecular Design* **2015,** 5, 25-56.
23. Caglič, D.; Krutein, M.C.; Bompiani, K.M.; Barlow, D.J.; Benoni, G.; Pelletier, J.C.; Reitz, A.B., et al. Identification of Clinically Viable Quinolinol Inhibitors of Botulinum Neurotoxin A Light Chain. *Journal of Medicinal Chemistry* **2014,** 57, 669-676.
24. Harrell Jr, W.A.; Vieira, R.C.; Ensel, S.M.; Montgomery, V.; Guernieri, R.; Eccard, V.S.; Campbell, Y., et al. A matrix-focused structure-activity and binding site flexibility study of quinolinol inhibitors of botulinum neurotoxin serotype A. *Bioorganic & Medicinal Chemistry Letters* **2017,** 27, 675-678.
25. Gómez-Jeria, J.S. On some problems in quantum pharmacology I. The partition functions. *International Journal of Quantum Chemistry* **1983,** 23, 1969-1972.
26. Gómez-Jeria, J.S. Modeling the Drug-Receptor Interaction in Quantum Pharmacology. In *Molecules in Physics, Chemistry, and Biology*, Maruani, J., Ed. Springer Netherlands: 1989; Vol. 4, pp 215-231.
27. Gómez-Jeria, J.S.; Ojeda-Vergara, M. Parametrization of the orientational effects in the drug-receptor interaction. *Journal of the Chilean Chemical Society* **2003,** 48, 119-124.
28. Gómez-Jeria, J.S. *Elements of Molecular Electronic Pharmacology (in Spanish)*. 1st ed.; Ediciones Sokar: Santiago de Chile, 2013.
29. Gómez-Jeria, J.S. A New Set of Local Reactivity Indices within the Hartree-Fock-Roothaan and Density Functional Theory Frameworks. *Canadian Chemical Transactions* **2013,** 1, 25-55.
30. Salgado-Valdés, F.; Gómez-Jeria, J.S. A Theoretical Study of the Relationships between Electronic Structure and CB1 and CB2 Cannabinoid Receptor Binding Affinity in a Group of 1-Aryl-5-(1-H-pyrrol-1-yl)-1-H-pyrazole-3-carboxamides. *Journal of Quantum Chemistry* **2014,** 2014 Article ID 431432, 1-15.
31. Martin, Y.C. *Quantitative drug design: a critical introduction*. M. Dekker: New York, 1978.
32. Peradejordi, F.; Martin, A.N.; Cammarata, A. Quantum chemical approach to structure-activity relationships of tetracycline antibiotics. *Journal of Pharmaceutical Sciences* **1971,** 60, 576-582.
33. Gómez-Jeria, J.S.; Flores-Catalán, M. Quantum-chemical modeling of the relationships between molecular structure and in vitro multi-step, multimechanistic drug effects. HIV-1 replication inhibition and inhibition of cell proliferation as examples. *Canadian Chemical Transactions* **2013,** 1, 215-237.
34. Gómez-Jeria, J.S.; Morales-Lagos, D. The mode of binding of phenylalkylamines to the Serotonergic Receptor. In *QSAR in design of Bioactive Drugs*, Kuchar, M., Ed. Prous, J.R.: Barcelona, Spain, 1984; pp 145-173.
35. Gómez-Jeria, J.S.; Morales-Lagos, D.R. Quantum chemical approach to the relationship between molecular structure and serotonin receptor binding affinity. *Journal of Pharmaceutical Sciences* **1984,** 73, 1725-1728.
36. Gómez-Jeria, J.S.; Morales-Lagos, D.; Rodriguez-Gatica, J.I.; Saavedra-Aguilar, J.C. Quantum-chemical study of the relation between electronic structure and pA2 in a series of 5-substituted tryptamines. *International Journal of Quantum Chemistry* **1985,** 28, 421-428.

37. Gómez-Jeria, J.S.; Cassels, B.K.; Saavedra-Aguilar, J.C. A quantum-chemical and experimental study of the hallucinogen (±)-1-(2,5-dimethoxy-4-nitrophenyl)-2-aminopropane (DON). *European Journal of Medicinal Chemistry* **1987,** 22, 433-437.
38. Gómez-Jeria, J.S.; Sotomayor, P. Quantum chemical study of electronic structure and receptor binding in opiates. *Journal of Molecular Structure: THEOCHEM* **1988,** 166, 493-498.
39. Gómez-Jeria, J.S.; Soto-Morales, F.; Larenas-Gutierrez, G. A Zindo/1 Study of the Cannabinoid-Mediated Inhibition of Adenylyl Cyclase. *Iranian International Journal of Science* **2003,** 4, 151-164.
40. Gómez-Jeria, J.S.; Soto-Morales, F.; Rivas, J.; Sotomayor, A. A theoretical structure-affinity relationship study of some cannabinoid derivatives. *Journal of the Chilean Chemical Society* **2008,** 53, 1393-1399.
41. Gómez-Jeria, J.S. A DFT study of the relationships between electronic structure and peripheral benzodiazepine receptor affinity in a group of N,N-dialkyl-2- phenylindol-3-ylglyoxylamides (Erratum in: J. Chil. Chem. Soc., 55, 4, IX, 2010). *Journal of the Chilean Chemical Society* **2010,** 55, 381-384.
42. Barahona-Urbina, C.; Nuñez-Gonzalez, S.; Gómez-Jeria, J.S. Model-based quantum-chemical study of the uptake of some polychlorinated pollutant compounds by Zucchini subspecies. *Journal of the Chilean Chemical Society* **2012,** 57, 1497-1503.
43. Bruna-Larenas, T.; Gómez-Jeria, J.S. A DFT and Semiempirical Model-Based Study of Opioid Receptor Affinity and Selectivity in a Group of Molecules with a Morphine Structural Core. *International Journal of Medicinal Chemistry* **2012,** 2012 Article ID 682495, 1-16.
44. Alarcón, D.A.; Gatica-Díaz, F.; Gómez-Jeria, J.S. Modeling the relationships between molecular structure and inhibition of virus-induced cytopathic efects. Anti-HIV and anti-H1N1 (Influenza) activities as examples. *Journal of the Chilean Chemical Society* **2013,** 58, 1651-1659.
45. Gómez-Jeria, J.S. A theoretical study of the relationships between electronic structure and anti-inflammatory and anti-cancer activities of a series of 6,7-substituted-5,8-quinolinequinones. *International Research Journal of Pure and Applied Chemistry* **2014,** 4, 270-291.
46. Gómez-Jeria, J.S. A quantum chemical analysis of the relationships between electronic structure, PAK1 inhibition and MEK phosphorylation in a series of 2-arylamino-4-aryl-pyrimidines. *SOP Transactions on Physical Chemistry* **2014,** 1, 10-28.
47. Gómez-Jeria, J.S. Toward Understanding the Inhibition of Vesicular Stomatitis Virus Replication in MDCK Cells by 4-Quinolinecarboxylic acid Analogues. A Density Functional Study. *Der Pharma Chemica* **2014,** 6, 64-77.
48. Gómez-Jeria, J.S. A Note on the Relationships between Electronic Structure and Inhibition of Chikungunya Virus Replication by a group of [1,2,3]Triazolo[4,5-d]pyrimidin-7(6H)-ones Derivatives. *Journal of Computational Methods in Molecular Design* **2014,** 4, 38-47.
49. Gómez-Jeria, J.S.; Molina-Hidalgo, J. A Short Note on the Relationships between Electronic Structure and S-Nitrosoglutathione Reductase Inhibition by 3-[1-(4-carbamoylphenyl)-5-phenyl-1H-pyrrol-2-yl]propanoic acids. *Journal of Computational Methods in Molecular Design* **2014,** 4, 1-9.
50. Pino-Ramírez, D.I.; Gómez-Jeria, J.S. A Quantum-chemical study of the in vitro cytotoxicity of a series of (Z)-1-aryl-3-arylamino-2-propen-1-ones against human tumor DU145 and K562 cell lines. *American Chemical Science Journal* **2014,** 4, 554-575.
51. Gómez-Jeria, J.S. A Theoretical Study of the Relationships between Electronic Structure and Antifungal Activity against *Botrytis cinerea* and *Colletotrichum lagenarium* of a Group of Carabrone Hydrazone Derivatives. *Research Journal of Pharmaceutical, Biological and Chemical Sciences* **2015,** 6, 688-697.
52. Gómez-Jeria, J.S.; Robles-Navarro, A. Quantum-chemical study of the cytotoxic activity of pyrimidine–benzimidazol hybrids against MCF-7, MGC-803, EC-9706 and SMMC-7721 human cancer cell lines. *Research Journal of Pharmaceutical, Biological and Chemical Sciences* **2015,** 6, 755-783.

53. Gómez-Jeria, J.S.; Robles-Navarro, A. A Quantum Chemical Study of the Relationships between Electronic Structure and cloned rat 5-HT_{2C} Receptor Binding Affinity in N-Benzylphenethylamines. *Research Journal of Pharmaceutical, Biological and Chemical Sciences* **2015,** 6, 1358-1373.
54. Gómez-Jeria, J.S.; Valdebenito-Gamboa, J. A Density Functional Study of the Relationships between Electronic Structure and Dopamine D_2 receptor binding affinity of a series of [4-(4-Carboxamidobutyl)]-1-arylpiperazines. *Research Journal of Pharmaceutical, Biological and Chemical Sciences* **2015,** 6, 203-218.
55. Gómez-Jeria, J.S.; Abarca-Martínez, S. A theoretical analysis of the cytotoxicity of a series of β-carboline-dithiocarbamate derivatives against prostatic cancer (DU-145), breast cancer (MCF-7), human lung adenocarcinoma (A549) and cervical cancer (HeLa) cell lines. *Der Pharma Chemica* **2016,** 8, 507-526.
56. Gómez-Jeria, J.S.; Castro-Latorre, P.; Kpotin, G. Quantum Chemical Analysis of the Relationships between Electronic Structure and Antiviral Activity against HIV-1 of some Pyrazine-1,3-thiazine Hybrid Analogues. *Der Pharma Chemica* **2016,** 8, 234-239.
57. Gómez-Jeria, J.S.; Moreno-Rojas, C. A theoretical study of the inhibition of human 4-hydroxyphenylpyruvate dioxygenase by a series of pyrazalone-quinazolone hybrids. *Der Pharma Chemica* **2016,** 8, 475-482.
58. Gómez-Jeria, J.S.; Salazar, R. A DFT study of the inhibition of FMS-like tyrosine kinase 3 and the antiproliferative activity against MV4-11 cells by N-(5-(tert-butyl)isoxazol-3-yl)-N'-phenylurea analogs. *Der Pharma Chemica* **2016,** 8, 1-9.
59. Kpotin, G.; Atohoun, S.Y.G.; Kuevi, U.A.; Kpota-Hounguè, A.; Mensah, J.-B.; Gómez-Jeria, J.S. A Quantum-Chemical study of the Relationships between Electronic Structure and Trypanocidal Activity against Trypanosoma Brucei Brucei of a series of Thiosemicarbazone derivatives. *Der Pharmacia Lettre* **2016,** 8, 215-222.
60. Robles-Navarro, A.; Gómez-Jeria, J.S. A Quantum-Chemical Analysis of the Relationships between Electronic Structure and Citotoxixity, GyrB inhibition, DNA Supercoiling inhibition and anti-tubercular activity of a series of quinoline–aminopiperidine hybrid analogues. *Der Pharma Chemica* **2016,** 8, 417-440.
61. Note. The results presented here are obtained from what is now a routinary procedure. For this reason, we built a general model for the paper's structure. This model contains *standard* phrases for the presentation of the methods, calculations and results because they do not need to be rewritten repeatedly. In.
62. Frisch, M.J.; Trucks, G.W.; Schlegel, H.B.; Scuseria, G.E.; Robb, M.A.; Cheeseman, J.R.; Montgomery, J., J.A., et al. *G03 Rev. E.01*, Gaussian: Pittsburgh, PA, USA, 2007.
63. Gómez-Jeria, J.S. *D-Cent-QSAR: A program to generate Local Atomic Reactivity Indices from Gaussian 03 log files. v. 1.0*, v. 1.0; Santiago, Chile, 2014.
64. Gómez-Jeria, J.S. An empirical way to correct some drawbacks of Mulliken Population Analysis (Erratum in: J. Chil. Chem. Soc., 55, 4, IX, 2010). *Journal of the Chilean Chemical Society* **2009,** 54, 482-485.
65. Gómez-Jeria, J.S. Tables of proposed values for the Orientational Parameter of the Substituent. I. Monoatomic, Diatomic, Triatomic, n-CnH2n+1, O-n-CnH2n+1, NRR', and Cycloalkanes (with a single ring) substituents. *Research Journal of Pharmaceutical, Biological and Chemical Sciences* **2016,** 7, 288-294.
66. Statsoft. *Statistica v. 8.0*, 2300 East 14 th St. Tulsa, OK 74104, USA, 1984-2007.
67. Fukui, K.; Fujimoto, H. *Frontier orbitals and reaction paths: selected papers of Kenichi Fukui*. World Scientific: Singapore; River Edge, N.J., 1997.
68. Klopman, G.; Hudson, R.F. Polyelectronic perturbation treatment of chemical reactivity. *Theoretica chimica acta* **1967,** 8, 165-174.
69. Klopman, G. Chemical reactivity and the concept of charge- and frontier-controlled reactions. *Journal of the American Chemical Society* **1968,** 90, 223-234.